

Enhancement of Heat Transfer over a Cylinder by Acoustic Excitation

J. H. Su* and C. Gau†

National Cheng Kung University, Tainan, Taiwan 70101, Republic of China

and

C. S. Yang‡

Far East College, Tainan, Taiwan 70101, Republic of China

Experiments were performed to demonstrate enhancement of heat transfer around a horizontal cylinder by the presence of acoustic excitation. The horizontal cylinder was heated uniformly and placed inside a wind tunnel. The wall temperatures around the cylinder were measured and are used to determine the local heat transfer in the circumferential direction. To avoid interference with the flow, the acoustic generator, which was a loud speaker, was placed downstream of the cylinder. The frequency of the sound F_e , was set equal to the natural frequency, F_n , of the shedding vortex in the wake or a multiple of F_n . Therefore, synchronization of vortex shedding with acoustic wave can be expected. The excitation frequencies selected were $F_e/F_n = 1, 2, 3$, up to 8. Other frequencies at $F_e/F_n = 1.5, 2.5, 3.5$, up to 7.5 were also selected for comparison. During the experiments, the sound pressure varied from 0 to 100 dB and the Reynolds number varied from 2938 to 8814. The heat transfer around the cylinder was found to be significantly enhanced by the acoustic waves. More detailed measurements for the energy spectrum of the acoustic waves generated by the current speaker were made. This provides a better understanding of the physical process. Flow visualization is also performed to demonstrate synchronization of vortex shedding with acoustic excitation. The effect of sound pressure levels and Reynolds numbers on the wall heat transfer are presented and discussed.

Nomenclature

D	= diameter of cylinder, cm
d	= diameter of thermocouple wire, cm
F_e	= excitation frequency of the sound, Hz
F_n	= natural shedding frequency of the vortex, Hz
h	= convective heat transfer coefficient, W/m ² K
I	= dc electric current, A
k	= thermal conductivity of air, W/m K
L	= formation length of vortex, cm
Nu	= local Nusselt number, hD/k
q	= heat flux, W/m ²
Re	= Reynolds number, $u_0 D/\nu$
S_{pl}	= sound pressure level, dB
St	= Strouhal number, $F_n D/u_0$
T	= temperature, K
T_e	= the period for complete cycle of vortex formation, $1/F_n$, s
t	= time, s
u	= velocity, m/s
V	= voltage, V
θ	= angle measured from the stagnation point, deg
ν	= kinematic viscosity, m ² /s

Subscript

av	= refers to average
o	= refers to freestream

stag	= refers to backward stagnation, i.e., 180 deg from the forward stagnation point
w	= refers to the wall of cylinder

I. Introduction

MOST high-temperature thermal devices under normal operation may encounter some degree of sound. The sound may be generated from the flow itself and/or some components in motion. This kind of acoustic waves usually are at small or large sound pressure with relatively low or high frequency. However, in the practical design of a thermal system, acoustic waves are not considered, and their effects on the wall heat transfer are neglected. Despite this fact, there are indeed some studies^{1–8} on heat transfer by acoustic waves. These reports considered cases when both the sound pressure level and the sound frequency were very high ($S_{pl} = 130$ – 160 dB; $F_e = 1000$ – 3000 or 6000 Hz) and so-called thermoacoustic streaming occurred. In these situations, the heat transfer process can be significantly enhanced. Different flow and heat transfer configurations have been considered, such as natural^{2–4} or forced⁵ convection from a heated horizontal cylinder, forced convection from a sphere,^{6,7} and natural convection from a vertical flat plate.⁸ For the case where the sound pressure level is less than 130 dB or where the sound frequency is low, thermoacoustic streaming is not significant enough to affect the heat transfer. However, the current study will demonstrate that, in the presence of acoustic waves at sound pressure levels less than 130 dB or when the sound frequency is low, heat transfer for flow over a heated cylinder can be significantly enhanced when the excitation frequency of the sound is properly selected and controlled.

This study is inspired by the results of previous studies^{9,10} which showed that small-amplitude ($A/D = 0$ – 0.064) vibration of a cylinder either in the streamwise or the transverse direction of the flow can have a significant effect on both the vortex flow structure and the heat transfer around the cylinder when the excitation frequency is the natural shedding frequency of the vortex or a multiple of this frequency. This is the condition when the cylinder's vibration is synchronized or locked in with shedding of the vortex. At this stage, the instability wave in the wake can be significantly

Received 2 August 2004; revision received 15 June 2005; accepted for publication 18 June 2005. Copyright © 2005 by the American Institute of Aeronautics and Astronautics, Inc. All rights reserved. Copies of this paper may be made for personal or internal use, on condition that the copier pay the \$10.00 per-copy fee to the Copyright Clearance Center, Inc., 222 Rosewood Drive, Danvers, MA 01923; include the code 0887-8722/06 \$10.00 in correspondence with the CCC.

*Graduate Student, Institute of Aeronautics and Astronautics.

†Professor, Institute of Aeronautics and Astronautics; gau@mail.ncku.edu.tw.

‡Associate Professor, Computer Application Engineering Department; cs0517@pchome.com.tw.

amplified, which leads to the result that the vortex can be initiated earlier. The vortex becomes stronger, and the vortex formation length can be significantly reduced.⁹ Vortex flow is expected to enhance the heat transfer behind the cylinder. However, Gau et al.^{8,9} found that under synchronization, enhancement of the heat transfer is found not only behind the cylinder, but also on the front side, i.e., at the stagnation point and in its downstream region. The enhancement in the total heat transfer is very large and can be more than half of the total heat input.

It can be expected that the instability wave in the wake of the flow can also be amplified by the acoustic wave if the frequency of the acoustics is set equal to the natural shedding frequency of the vortex or a multiple of this frequency. Therefore, synchronization of vortex shedding with acoustic waves, which leads to earlier formation of the vortex and enhancement of the heat transfer around the cylinder, can also be expected. Current experiments demonstrate how the heat transfer around a heated cylinder can be affected or enhanced when an acoustic wave is present in the flow and is synchronized with the shedding frequency of the vortex in the wake. A synchronization frequency of the sound wave at the natural shedding frequency of the vortex or a multiple (integer) of this frequency is selected: i.e., $F_e/F_n = 1, 2, 3, \dots$, up to 8. For comparison, acoustic excitation at nonharmonic frequencies, such as $F_e/F_n = 1.5, 2.5, \dots$, up to 7.5, which may be partially synchronized with vortex shedding, is also selected. During the experiments, the Nusselt number around the cylinder will be measured as the Reynolds number varies from 2938 to 8814. The enhancement of the heat transfer at different excitation frequencies and sound pressure levels is presented and discussed.

II. Experimental Apparatus and Procedure

The cylinder is a 50-cm-long and 0.3-cm-thick Bakelite tube that has an outside diameter of 3 cm. The purpose of selecting a thin Bakelite tube is, first, to reduce both the radial and the circumferential conduction of heat, and second, to maintain a certain kind of rigidity that causes no deformation during experiments. To further reduce the circumferential conduction of heat, a 0.05-cm-thick rubber tube is used to cover the cylinder. This makes the outside diameter of the cylinder 3.1 cm. A 0.015-mm-thick stainless steel foil is glued on the tube. The electrodes are made small. They are fixed at the ends of the tube that extend outside the wind tunnel. After electric current is passed through the foil, the cylinder's surface can be heated uniformly at desired heat flux conditions. The tube ends are sealed with formed rubber for insulation. The total heat

loss to the ambient, which includes both the conduction loss along the cylinder wall and the radiation loss directly from the steel foil, is estimated to be less than 2%.

The cylinder is placed horizontally (perpendicular to the direction of the gravitational force), as shown in Fig. 1, in the test section of a wind tunnel that has a cross section of 30×30 cm. The wind tunnel can provide a uniform air flow over the cylinder with a turbulence intensity less than 0.7. The freestream velocity in the wind tunnel was measured with a Pitot tube.

The excitation system is a low-frequency-range speaker that is mounted approximately $10D$ downstream of the cylinder and is on the upper wall outside the wind tunnel system, as shown in Fig. 1. This speaker is driven by a function generator that provides sine wave signals at desired frequencies. The sine wave signals are monitored with an oscilloscope and are amplified to desired levels before entering the speaker. The acoustic waves generated by the speaker can propagate into the air flow through the holes in the wall of the wind tunnel. The waves can move upstream and pass through the vortex formation region and the cylinder. To analyze the acoustic waves, a microphone is placed on the back of the cylinder to acquire the wave signals. The wave signals are then sent to a personal computer for Fourier spectrum analysis. The spectrum of the acoustic waves is computed and obtained by means of the fast Fourier transform technique. The sound pressure at the upper point of the cylinder is measured with a sound-level meter made by the B&K Co. and is controlled at desired levels by the amplifier. The meter has measurement accuracy within 0.5 dB. To reduce the noise generated by the motor and the blower, they are placed far upstream of the test section. In addition, the airstream is fed into a noise reduction chamber before entering into the settling chamber. The noise reduction chamber is made up of many air passages with a wavy sponge as a noise absorber. In this way the background noise level in the wind tunnel is reduced and is maintained near 43 dB in the current study.

The wall of the test section is made of Plexiglas to allow flow visualization. Flow visualization by smoke generation is facilitated by a thin electrically heated wire coated with oil. This thin wire is inserted vertically across the cross section of the wind tunnel, as shown in Fig. 1, and is at approximately $10D$ upstream of the cylinder. Due to surface tension, a small amount of oil drops down slowly along the wire from an oil pan in the top of the wind tunnel and is vaporized upon heating. To avoid turbulence generation, which can dissipate the smoke rapidly, the velocity of the flow remains relatively low ($Re = 1900$) during the flow visualization experiments. Because the wire is very thin and is far from the cylinder, it could not affect the

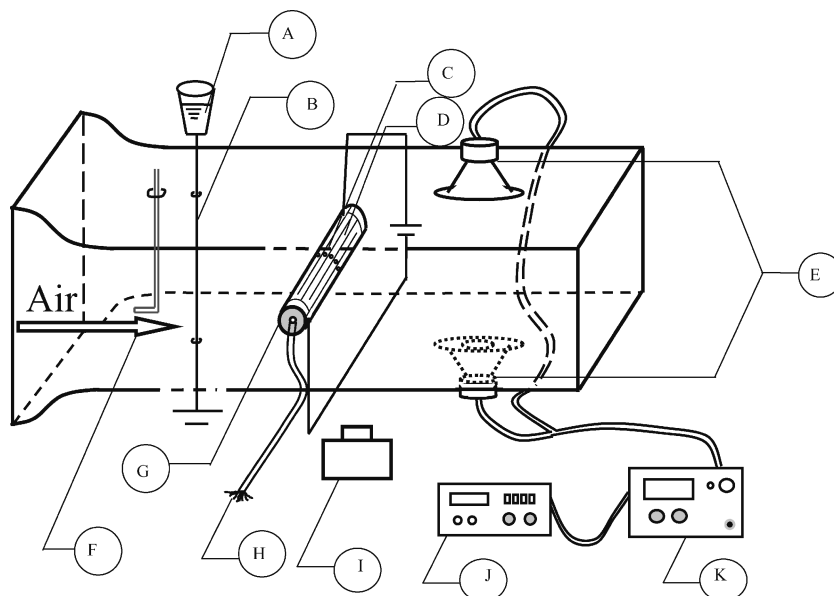


Fig. 1 Schematic diagram of the experimental setup: (A) oil pan, (B) electric resistor, (C) thermocouples, (D) stainless steel foil, (E) speaker, (F) Pitot tube, (G) cylinder, (H) thermocouple and electric wires, (I) camera, (J) function generator, and (K) amplifier.

upstream flow conditions. The smoke follows the streamline of the flow, and its pattern can be clearly visualized and photographed, as shown in a later section.

To measure the circumferential temperature distribution around the cylinder wall, a total of 30 K-type thermocouples were inserted individually into equally spaced small holes drilled in the tube wall in so that the thermocouple junction could attach to the heated steel foil. These thermocouples are located in the center along the length of the tube. All the thermocouple junctions are coated with epoxy to avoid electric contact with the foil. The thermocouple wires used have a very small diameter, $d = 0.05$ mm. To check the axial conduction loss along the cylinder wall, some additional thermocouples are embedded in the tube wall close to the ends. All the temperature signals are acquired with a data logger and sent into a personal computer for data processing and plotting. Before the experiments, all thermocouples are calibrated in a constant-temperature bath to ensure a measurement accuracy of $\pm 0.1^\circ\text{C}$.

To ensure that the stainless steel foil is heated uniformly, the entire foil is cut into a number of long strips that are axial. The strips are smoothly glued onto the tube wall. There is no waviness or overlapping of foil strips. Each strip is heated individually with an equal amount of dc power. With the desired voltage V and current I passing through the thin strip, the heat flux along the surface can be calculated and is equal to $V I / A$, where A is the area of the strip. The local heat transfer coefficient can be determined with the equation

$$h = q / (T_w - T_o) \quad (1)$$

The uncertainty of the experimental data obtained in the present system is determined according to the procedure outlined by Kline and McClintock.¹⁰ It is found that the maximum uncertainty in the local Nusselt number is 3.5%, whereas the Reynolds number is 5.7%.

From the correlations listed in past work,^{11,12} the Strouhal number of the vortex, which is equal to $F_n D / u_0$, in the current experimental range of the Reynolds number covered was $St = 0.194$. Therefore, the shedding frequency of the vortex can be calculated at a given flow speed and a known diameter of the cylinder. The calculated shedding frequencies agree well with the ones obtained from our experimental observations. Therefore, the previous correlation was adopted to find the shedding frequencies of the vortices in the present work.

During the experiments, the frequencies of acoustic excitation were selected at 1, 1.5, 2, 2.5, 3, and up to 8 times the natural shedding (Strouhal) frequency of the vortices. In this way, one can examine the effect of acoustic excitation on the flow and heat transfer at the harmonic frequency $F_e/F_n = 1$, the superharmonic frequencies $F_e/F_n = 2, 3, 4$, and up to 8, and the nonharmonic frequencies $F_e/F_n = 1.5, 2.5$, up to 7.5.

III. Results and Discussion

A. Flow Visualization

In general, the current flow visualization results indicate that at superharmonic or nonharmonic excitation, only the antisymmetric type of vortex formation can occur; that is, vortex shedding on either the upper or the lower sides of the cylinder occurs and grows alternately. The other type of vortex formation, the symmetric type, rarely occurs. It is noted that for the symmetric case, vortex shedding on both the upper and the lower sides of the cylinder occurs and grows simultaneously. This is somewhat different from the cases⁹ where a cylinder is under vibration at different frequencies. The occurrence of different types of vortex formation depends very much on the oscillation frequency and amplitude of the cylinder. The antisymmetric mode occurs most of the time at lower values of excitation ($F_e/F_n = 1.5$), while the symmetric mode occurs most of the time at higher values ($F_e/F_n = 2.5$). At $F_e/F_n = 1$, switching between symmetric and antisymmetric modes occurs frequently. Under acoustic excitation, however, no switching between these two modes occurs.

In addition, under acoustic excitation, the shedding frequency of the vortex does not vary with the excitation frequency of the sound, and is maintained at the natural shedding frequency (or the Strouhal frequency) F_n of the vortices. This finding is completely

different from the results of Blevins,¹² who reported that when the sound excitation is close to the vortex shedding frequency, the sound excitation was found to control the vortex shedding at a much higher sound pressure level. In the following presentation, instead of the complete cycle, only the vortex structures at two particular instants, $t/T_e = 0.216$ and 0.432 , are presented and compared with each other at different excitation frequencies.

When there is no acoustic excitation, the vortex formation process in the wake region is shown in Fig. 2a. The formation of a vortex is due to the exponential growth of small disturbances in the shear layer where the dominant mode of (fundamental) frequency is the shedding frequency F_n of the vortices.¹³ When an acoustic wave is generated at harmonic or superharmonic frequencies, the small disturbances can be greatly amplified, and the vortices can be initiated and formed in an earlier stage. This is the so-called synchronization or lock-in of vortex shedding due to acoustic excitation. The formation length of the vortex can be shortened greatly, as shown in Figs. 2b, 2c, and 2d. The formation lengths of the vortex at different excitation frequencies are measured and are clearly presented in Fig. 3 for $t/T_e = 0.216$ and 0.432 . The formation length here is defined as the distance measured from the center of the

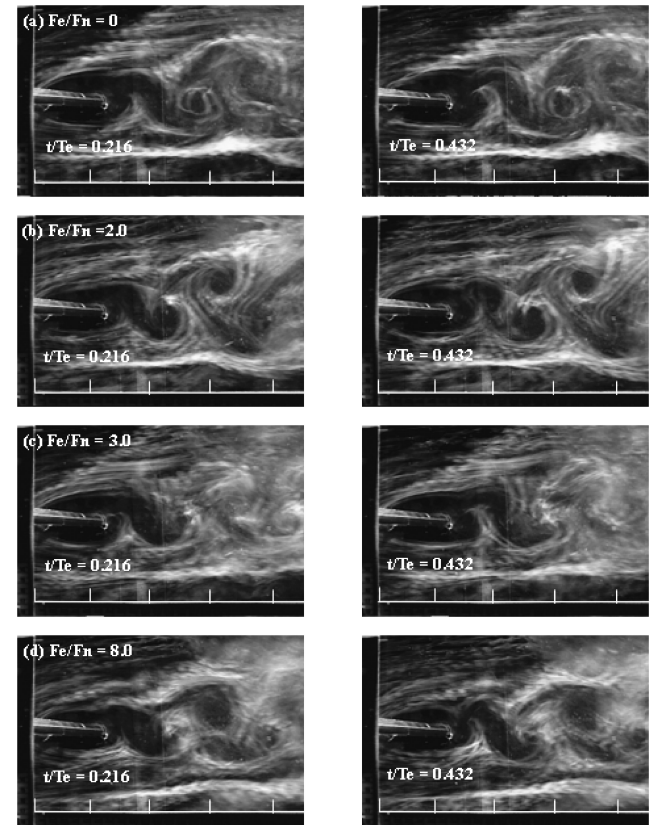


Fig. 2 Vortex structure at $t/T_e = 0.216$ and 0.432 for $Re = 1900$, $S_{pl} = 100$ dB, and a) $F_e/F_n = 0$, b) $F_e/F_n = 2$, c) $F_e/F_n = 3$, and d) $F_e/F_n = 8$.

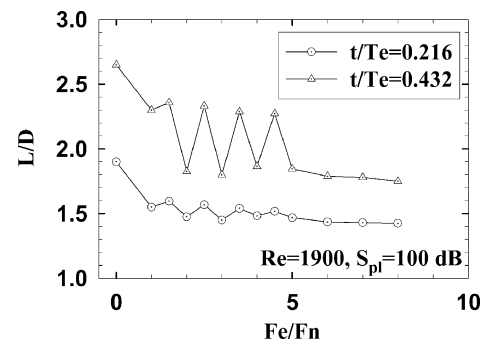


Fig. 3 Vortex formation lengths at different sound frequencies.

cylinder to the apex of the vortex. The maximum uncertainty for the formation length is 0.25% in single measurements. It appears that synchronization of vortex shedding with acoustic excitation occurs when the excitation frequency is harmonic or superharmonic, that is, whenever F_e/F_n is an integer. This is different from the case of cylinder oscillation, where complete synchronization of vortex shedding with cylinder oscillation occurs at $F_e/F_n = 1$ and 3 for cylinder oscillation in the transverse direction of the flow,⁹ while synchronization occurs at $F_e/F_n = 2$ for cylinder oscillation in line with the flow.¹⁰

It appears that, as long as acoustic excitation can be completed in one cycle of vortex shedding, synchronization of vortex shedding with acoustic waves occurs. However, the level of synchronization of vortex shedding with acoustic waves is expected to be different at different sound frequencies. The general trend should be that, as more acoustic energy is put into the unstable wave, that is, increase the sound frequency increases, this leads to an increase in the level of synchronization of vortex shedding with sound frequency. The increase in the level of synchronization of vortex shedding with sound frequency leads to a decrease in the formation length of the vortex. That is, the formation length of the vortex decreases with increasing sound frequency. Figure 3 shows this trend, especially for the case of $t/T_e = 0.423$, which is more interesting because it is closer to the end of vortex formation. However, this is not true for the case when $F_e/F_n = 4$ or 5. This peculiar phenomenon is attributed to the reduction in the intensity of the dominant mode of the superharmonics in the acoustic waves, and is discussed in a later section on the spectrum analysis of the acoustic waves. One can expect that the earlier formation of a vortex can greatly increase the heat transfer, especially behind the cylinder. This is discussed in the following section. For sound excitation at nonharmonic frequencies, that is, when F_e/F_n is not an integer, the vortex formation length is also shortened, as shown in Fig. 3, but not as much as for the harmonic or superharmonic cases. One can expect that the intense activity of vortex formation in the close vicinity of the cylinder can still enhance the heat transfer in that region, but the enhancement is again smaller.

B. Heat Transfer

The current heat transfer data were validated^{9,14} by comparing our data with those obtained from the literature, as shown in Fig. 4, when acoustic excitation is absent. The Nusselt number results were divided first by $Re^{0.5}$. It has been shown^{9,14} that, at the stagnation point or in the region before separation occurs, the Nusselt number results at different Reynolds numbers collapse into a single line, and the heat transfer parameter $Nu/Re^{0.5}$ at the stagnation point approaches 0.95. It appears that the current data not only show the same trend, but also agree very well with the data measured by Krall and Eckert.¹⁴ In Fig. 4, one can clearly see that the minimum heat

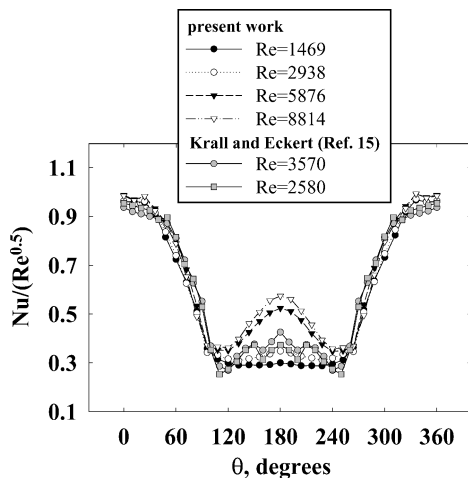


Fig. 4 Comparison of the Nusselt number distribution to the results of others without acoustic excitation.

transfer occurs approximately at $\theta = 120$ deg, which is expected to be the point of separation for a turbulent boundary layer around the cylinder as found in previous work.¹⁴ The data from Krall and Eckert show the same trend at a higher Reynolds number, $Re = 3570$. For a lower Reynolds number, when the boundary layer around the cylinder is in the transition or laminar region, however, the minimum in the heat transfer is expected to shift upstream.

In the wake region after flow separation occurs, however, the heat transfer parameter $Nu/Re^{0.5}$ at different Reynolds numbers does not collapse into a single line. This is attributed to the formation of vortex flow behind the cylinder, which has a significant effect on heat transfer in this region. It has been found^{15–17} that the formation length of the vortex, L/D , varies with Reynolds number and becomes shorter as Reynolds number increases. A shorter length of vortex formation can make the vortex closer to the back of the cylinder, which can significantly enhance heat transfer. Therefore, a higher heat-transfer parameter $Nu/Re^{0.5}$ can be found at higher Reynolds number, as shown in Fig. 4. Oscillation in the data of Krall and Eckert in the wake region is attributed to the much smaller cylinder used. The cylinder diameter in their work is 4.73 mm. The smaller cylinder diameter makes the formation length of the vortex, L , in the work of Krall and Eckert much shorter than that in the current work. The smaller vortex and formation closer to the cylinder causes oscillation in their data.

In the presence of acoustic excitation, synchronization of vortex shedding with the acoustic wave can significantly increase the heat transfer behind the cylinder, as shown in Fig. 5a. In addition, the enhancement normally increases with increasing the synchronization frequency F_e/F_n . This is clearly attributed to the earlier formation of the vortex at a higher excitation frequency that the vortex flow is closer to the cylinder. This can significantly enhance the heat transfer behind the cylinder. The higher the synchronization frequency, the greater the amount of excitation energy that is put into the vortex layer, and the earlier the formation of the vortex can be expected, as indicated in the flow visualization experiments for vibration excitation.^{9,10}

However, the heat transfer in the region before flow separation occurs is not affected at all, as shown in Fig. 5, by the earlier formation of vortices, or by the acoustic excitation. It appears that synchronization of vortex shedding with acoustic excitation does not affect either the heat transfer or the flow on the front side of the cylinder. Similar synchronization of vortex shedding that causes earlier formation of vortices and enhancement of heat transfer is found with cylinder oscillation either in the streamwise¹⁰ or the transverse⁹ direction of the flow. However, enhancement in the heat transfer is found not only on the back but also on the front of the cylinder, that is, in the region before flow separation occurs. This was attributed to the fact that the instability wave that causes earlier formation of vortices is initiated and amplified by the cylinder's oscillation in the very near field upstream region, that is, at the stagnation point.

In the current synchronization of a vortex with sound cases, it appears that the instability wave is amplified directly by the acoustic wave only in the region after flow separation occurs. It is noted that the flow in the region after separation occurs is highly unstable, whereas that in the upstream region before flow separation occurs is very stable, except at the stagnation point. It appears that, in the presence of acoustic excitation, the instability wave is amplified only in the unstable-flow region, not at the stagnation point, which is highly unstable-flow. This may be attributed to the location of the speaker behind of the cylinder. Therefore, it is suspected that the acoustic waves coming from behind the cylinder are blocked and cannot reach the front, that is, the stagnation point, of the cylinder. Further measurements on the acoustic wave at the stagnation point are necessary to clarify this argument. However, this will require a tiny microphone that can be placed at the stagnation point.

An increase in heat transfer with synchronization frequency does not always occur. At certain synchronization frequencies, enhancement in the heat transfer may be reduced, as shown more clearly in Fig. 5a, where the heat transfer for $F_e/F_n = 4$ or 5 is much less than that for $F_e/F_n = 3$. This is attributed to the current speaker used, which can generate many superharmonics, of which only

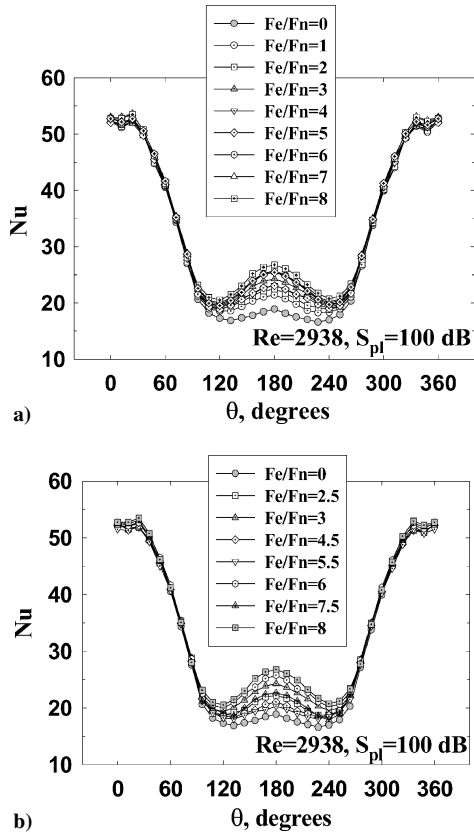


Fig. 5 Nusselt number distribution for $Re = 2938$ with acoustic excitation at $S_{pl} = 100$ dB for a) F_e/F_n from 0 to 8 and b) F_e/F_n at inharmonic frequencies.

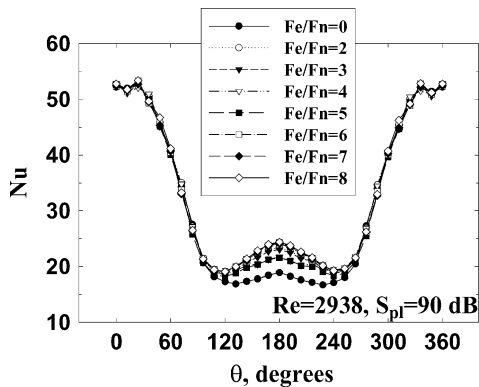


Fig. 6 Nusselt number distribution around a cylinder for $Re = 2938$ with acoustic excitation at $S_{pl} = 90$ dB.

the dominant mode becomes responsible for flow excitation. The spectral energy for the dominant mode of the superharmonics at $F_e/F_n = 4$ or 5 becomes less than that at $F_e/F_n = 3$. This causes less flow excitation at $F_e/F_n = 4$ or 5 than at $F_e/F_n = 3$. Similarly, the spectral energy for the dominant mode of the superharmonics at $F_e/F_n = 7$ becomes less than that at $F_e/F_n = 6$. This causes less flow excitation and less heat transfer enhancement at $F_e/F_n = 7$ than at $F_e/F_n = 6$. An additional detailed explanation will be given in a later section on the acoustic spectrum measurements.

As sound pressure level decreases, enhancement in the heat transfer decreases, as shown in Fig. 6 for $S_{pl} = 90$ dB. This is attributed to a decrease in the excitation energy that causes much later vortex initiation and decreased enhancement in the heat transfer. For $S_{pl} = 80$ dB, enhancement in the heat transfer is very similar to that shown in Fig. 6, but the enhancement is much less.¹⁸ Enhancement in the heat transfer actually decreases with decreasing sound pressure level or excitation energy. However, the trend in enhance-

ment with excitation frequency is very similar among the cases $S_{pl} = 100, 90$, and 80 dB. For example, heat transfer with excitation at $F_e/F_n = 5$ is also less than that at $F_e/F_n = 3$. In addition, heat transfer at $F_e/F_n = 8$ reaches a maximum. It appears that the relative importance of each of the excitation frequencies for heat transfer does not change with sound pressure level.

When the acoustic wave is not completely synchronized with vortex shedding, that is, F_e/F_n is not an integer, it may be partially synchronized. For example, when $F_e/F_n = 0.5, 1.5$, or 2.5 , synchronization with vortex shedding can occur every two, three, or five cycles of the acoustic wave. This can also lead to earlier formation of vortices and enhancement of heat transfer. Similar kinds of partial synchronization with vortex shedding have also been found in vibration excitation of cylinders.^{9,10} However, enhancement in heat transfer for partial synchronization is much less than that for the case of complete synchronization. Figure 5b shows that the heat-transfer enhancement for excitation at $F_e/F_n = 2.5$ is much less than at $F_e/F_n = 2$. However, the Nusselt number for excitation at $F_e/F_n = 4.5$ or 7.5 is much reduced and is even less than that at $F_e/F_n = 4$ or 7 . The reason for a larger Nusselt number existing at $F_e/F_n = 2.5$ than at $F_e/F_n = 4.5$ is not clear until the energy spectrum of the acoustic wave is measured and presented in the next section.

C. Energy Spectrum of the Sound

When sound is generated from a speaker at a given sound-pressure level, with frequency controlled by a function generator, sound may be reflected by the irregular surface of the wall, which can cause echoes. Interaction of echoes from walls at different locations can cause the sound waves to spread at many frequencies. In addition, the speaker or electrical system may also generate harmonics and noise. The actual sound that arrives at the flow around a cylinder may possess many frequencies. The energy spectrum of the sound that arrives in the vicinity of the cylinder should be measured to acquire the actual excitation frequencies and the sound pressure levels at each frequency.

1. Complete Synchronization of Vortex Shedding with the Sound Waves

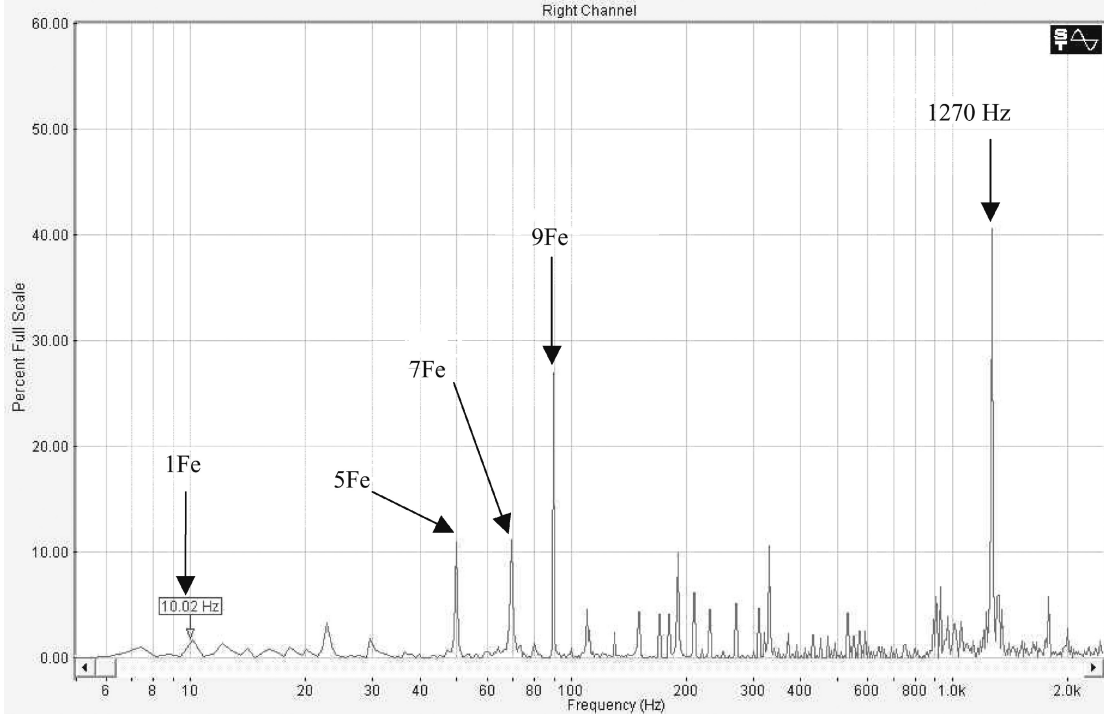
The complete synchronization of vortex shedding with acoustic waves means that, in every cycle of vortex shedding, there is more than one cycle of the excitation wave, and that the ratio F_e/F_n is an integer. The energy spectrum measured for sound generated at frequencies F_e/F_n from 0 to 8 and a sound pressure level of 100 dB are shown in Fig. 7 for $F_n = 10$ Hz. Measurements are also performed for the case when there is no sound excitation. The energy spectrum for this case is negligibly small. This result confirms not only that the background noise is negligibly small, but also that the entire microphone system used to receive the acoustic signals does not generate noise during measurements. However, when sound is generated at $F_e/F_n = 1$ to 2, the energy of sound waves at these frequencies is extremely low as compared with the energy at higher frequencies. Most of the spikes at higher frequencies are superharmonics (multiples) of the excitation, except for the spike at 1270 Hz, which is believed to be the noise generated by the speaker. In other words, the energy of the sound waves at these frequencies has been split into sound waves with many superharmonics and noise, as shown in Figs. 7a to 7d. After a careful check, it appears that these superharmonics or noise are not generated from the circuitry of the excitation system or echoes from the walls. They are actually generated by the speaker itself and are a characteristic of the current speaker used.

It is noted that in theory, each of the superharmonics can be used for synchronization with the natural shedding frequency of the vortex except for the noise. In practice, however, only the dominant mode of the superharmonics, that is, the one with the largest energy level, can be used for synchronization with vortex shedding. Other modes of the superharmonics can be treated as noise and can be neglected. Therefore, one can infer the relative amount of energy that can be used for excitation and synchronization with vortex shedding from the intensity of the superharmonic with the largest energy (spike) in comparison with the intensity of the noise at 1270 Hz. The excitation energy used for synchronization with

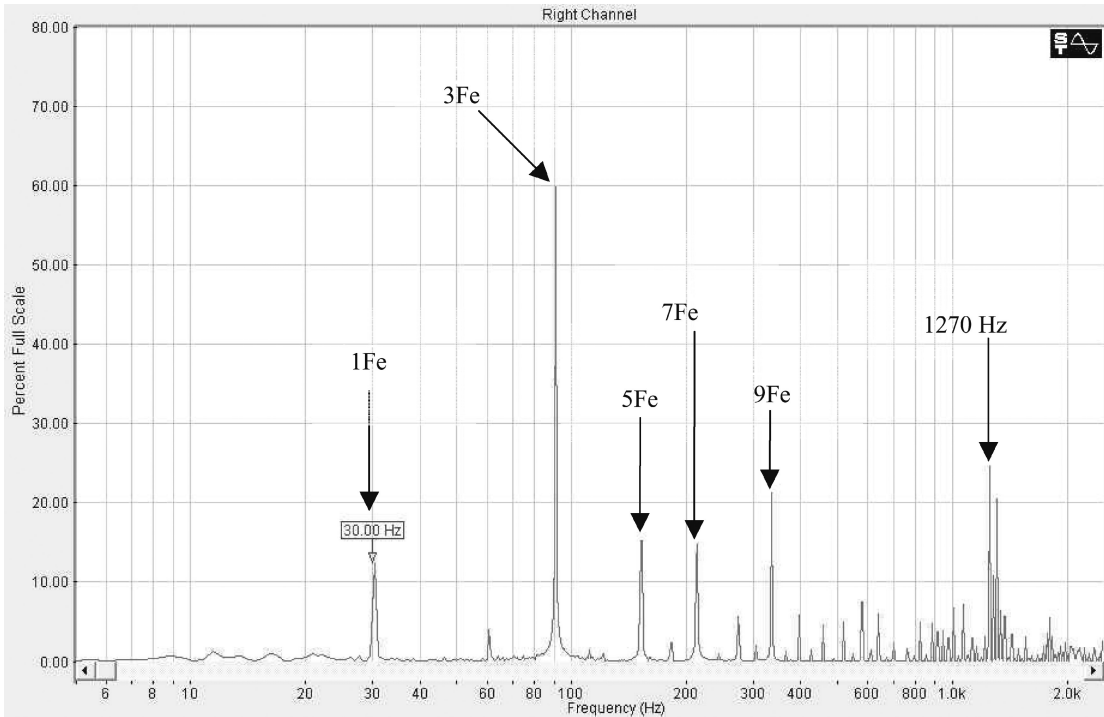
vortex shedding is large when the intensity of the dominant mode of the superharmonics is greater than the intensity of the noise. On the contrary, the excitation energy used for synchronization with vortex shedding is small when the intensity of the dominant superharmonic is less than the intensity of the noise. One exception is the excitation at $F_e/F_n = 1$ (for $F_n = 10$ Hz), where the spike at 1270 Hz can be viewed as a superharmonic of the excitation.

Experimental results indicate that the intensity of the dominant mode of the superharmonics increases with excitation frequency until $F_e/F_n = 3$, as shown in the form of typical results in Fig. 7a and

7b, but decreases, as shown in Fig. 7c, thereafter until $F_e/F_n = 5$. The increase in the intensity of the dominant mode can lead to earlier formation of vortices that can significantly increase the heat transfer. For $F_e/F_n = 7$, the intensity of the noise at 1270 Hz is very high as compared with the intensity of the excitation frequency at $F_e/F_n = 7$, implying that the excitation energy has been dissipated into noise. The energy used for synchronization with vortex shedding is relatively low. At $F_e/F_n = 8$, the excitation frequency becomes the dominant mode, and its intensity is several order of magnitude larger than its superharmonics and the noise, as shown

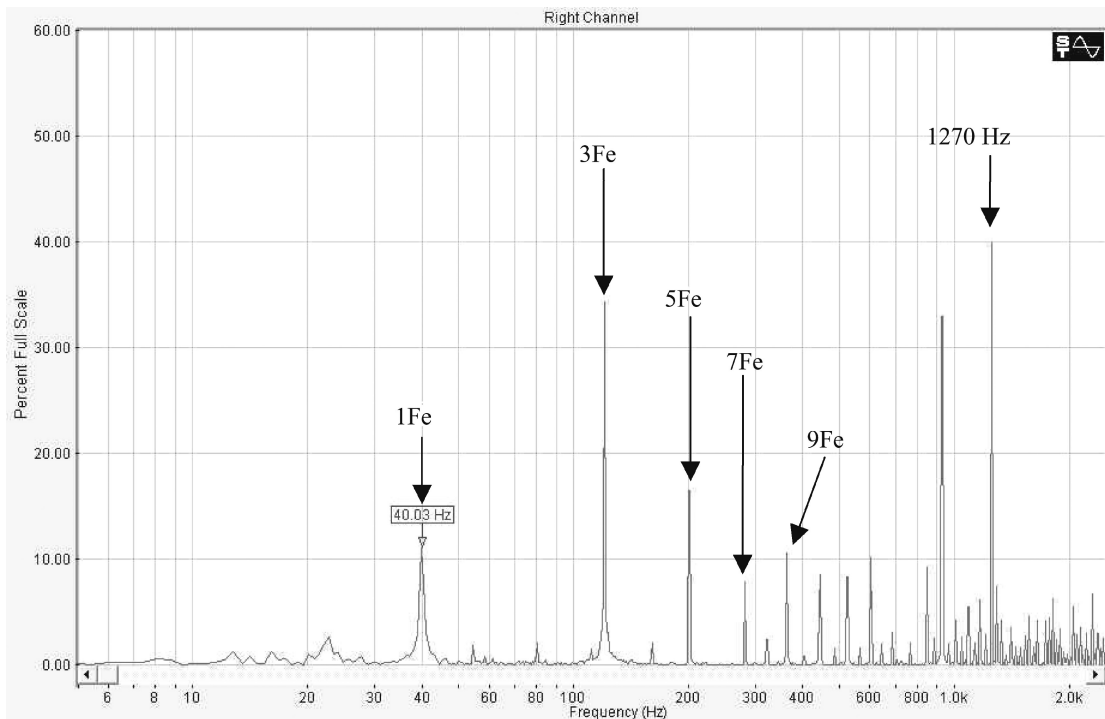


a)

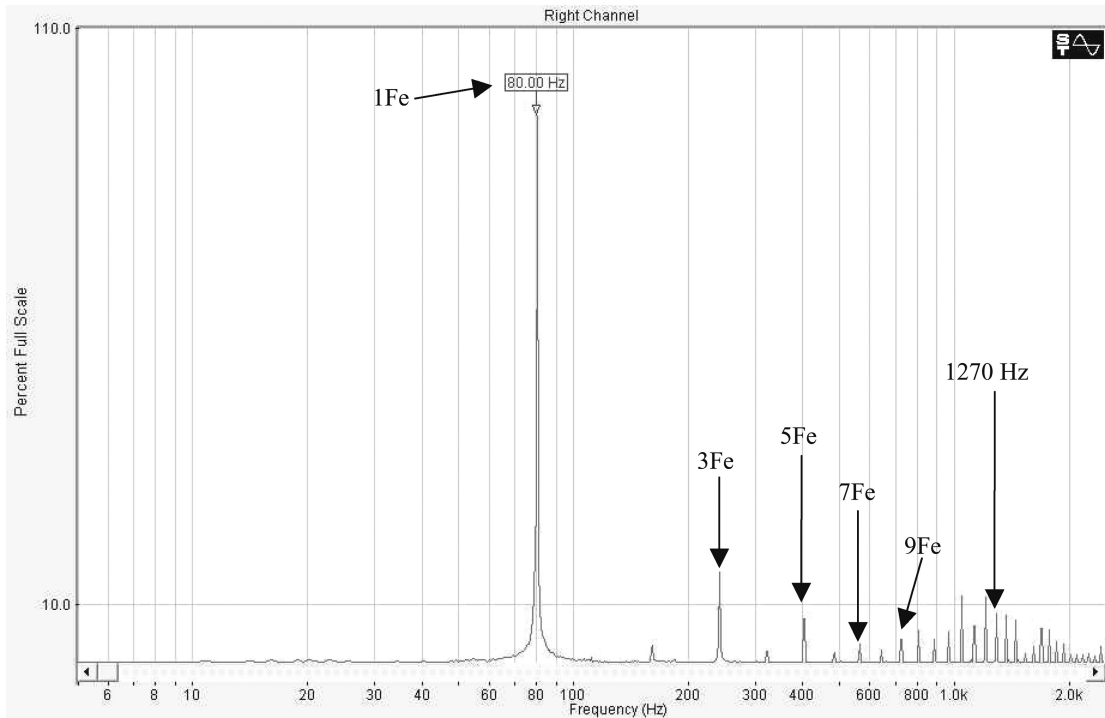


b)

Fig. 7 Energy spectrum of acoustic waves generated by a speaker for $Re = 2938$ and $F_n = 10$ Hz and a) $F_e/F_n = 1$, b) $F_e/F_n = 3$, c) $F_e/F_n = 4$, and d) $F_e/F_n = 8$.



c)



d)

Fig. 7 Energy spectrum of acoustic waves generated by a speaker for $Re = 2938$ and $F_n = 10$ Hz and a) $F_e/F_n = 1$, b) $F_e/F_n = 3$, c) $F_e/F_n = 4$, and d) $F_e/F_n = 8$ (continued).

in Fig. 7d. That means that most of the excitation energy is used for synchronization with vortex shedding. This explains that excitation at $F_e/F_n = 8$ can cause much earlier the vortex formation, and heat transfer enhancement is much greater than excitation at other frequencies.

2. Partial Synchronization of Vortex Shedding with Sound Waves

The energy spectrum of the acoustic waves for the case of partial synchronization of vortex shedding with sound waves is shown in Figs. 8a to 8d. The intensity of the dominant mode, at 3 or 5 F_e/F_n ,

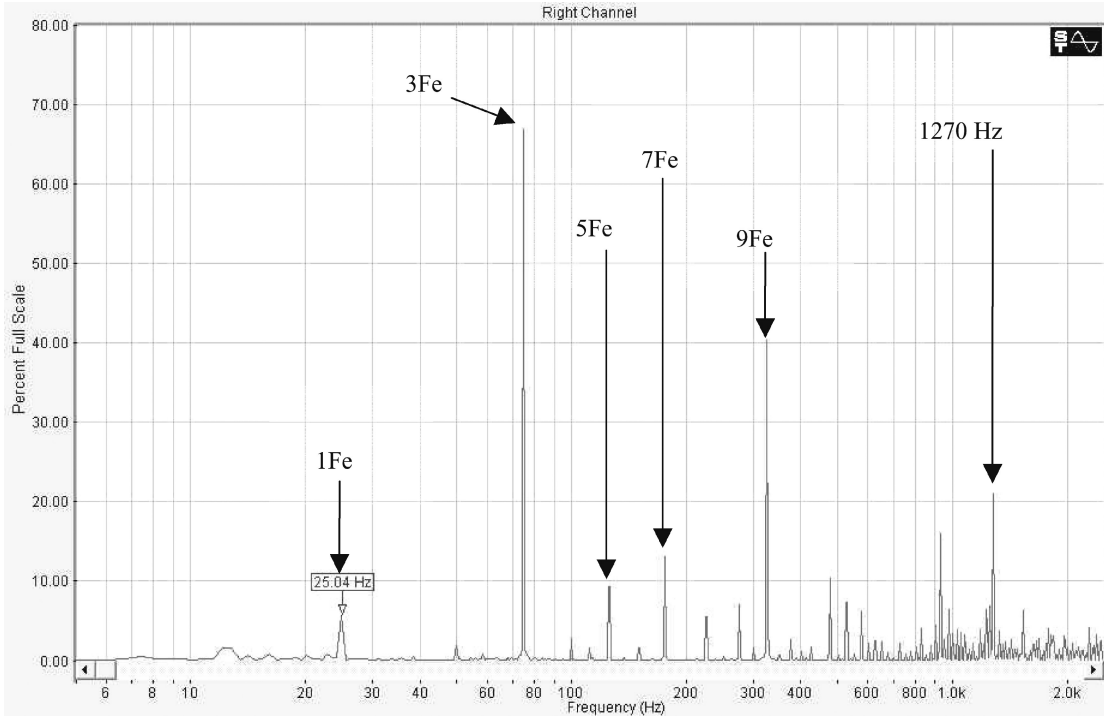
of the superharmonics increases significantly at $F_e/F_n = 2.5$ or 6.5, which appears to be due to the characteristics of the present speaker. This can lead to much earlier formation of a vortex behind the cylinder, which can significantly increase the heat transfer, as shown in Fig. 5b regarding the heat transfer measurements of the previous section. The intensity of the dominant mode at $F_e/F_n = 4.5$, 5.5, or 7.5 is much less than that at $F_e/F_n = 6.5$ or 2.5. Therefore, this reduced excitation energy explains the much smaller enhancement in the heat transfer presented in the previous section, as shown in Fig. 5b. It is very clear that the very large intensity of the noise at

1270 Hz for $F_e/F_n = 7.5$ does not contribute to any of the enhancement in the heat transfer, as shown in Fig. 5b.

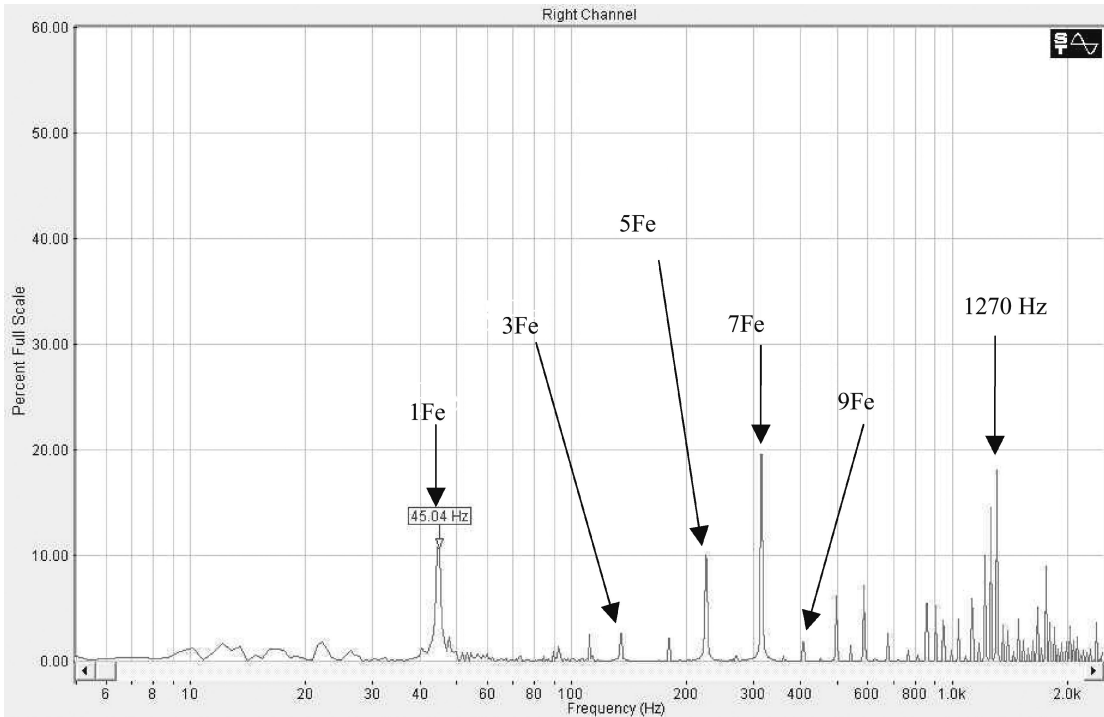
D. Further Discussion of Heat Transfer

At higher Reynolds number, synchronization of acoustic waves with vortex shedding can still be expected when F_e/F_n becomes integer. This can lead to a significant increase in the heat transfer, as shown in Fig. 9 for $Re = 5876$. Similarly, there is a large enhancement in the heat transfer at $F_e/F_n = 8$, and a much smaller enhancement in the heat transfer at $F_e/F_n = 4$ or 5 for $Re = 2938$ is

observed in this figure. However, enhancement in the heat transfer at $F_e/F_n = 6$ or 7 is very large and is very close to that of the case for $F_e/F_n = 8$. This is very different from the case for $Re = 2938$. This difference is attributed to the excitation of the speaker at much higher frequencies for $Re = 5876$. The energy spectrum of the acoustic wave generated from the speaker at higher excitation frequencies is expected to be different from that at lower excitation frequencies. Different energy spectra of the acoustic waves generated by the speaker can cause variation in the heat transfer at different excitation frequency ratios F_e/F_n .

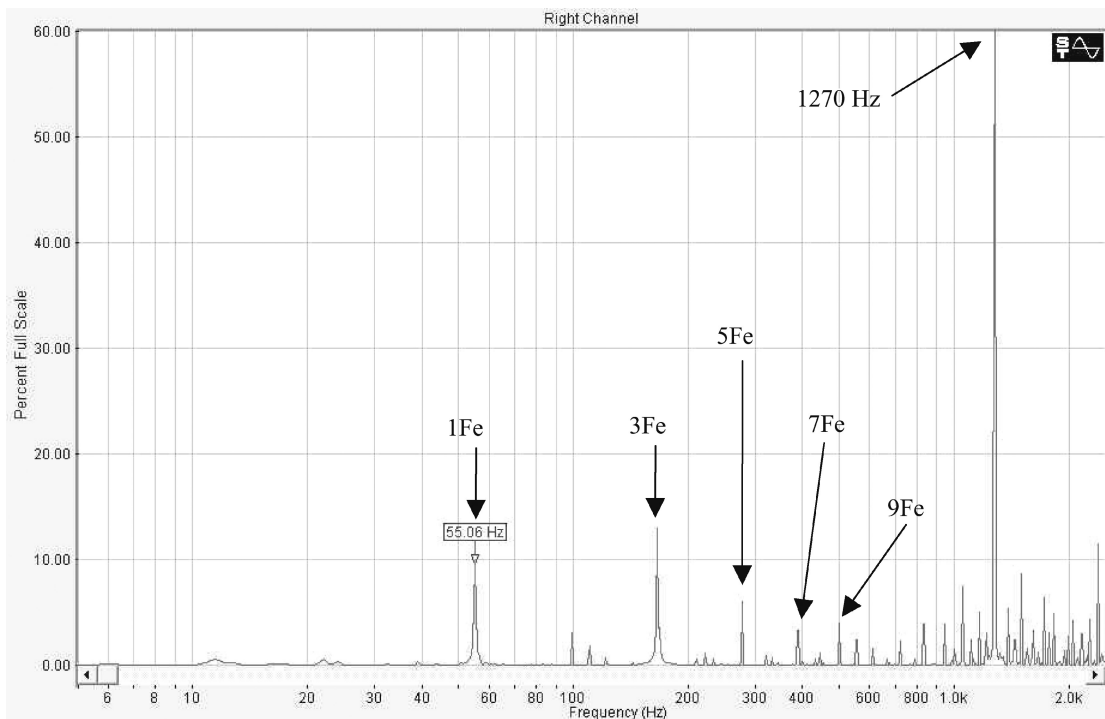


a)

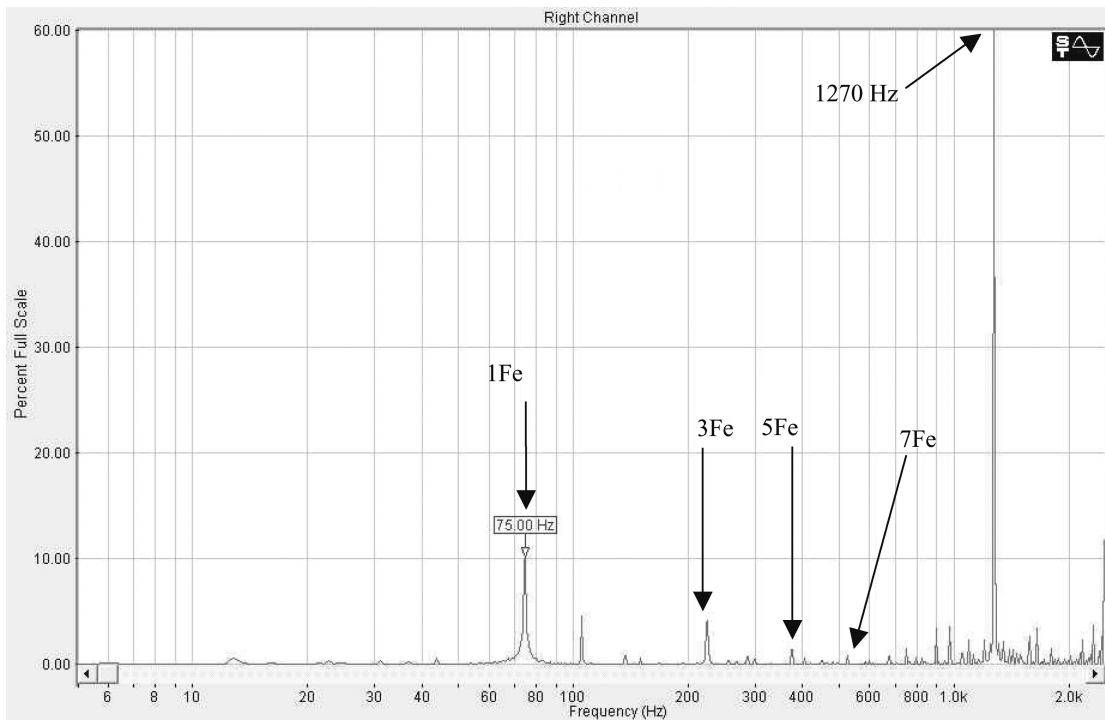


b)

Fig. 8 Energy spectrum of acoustic waves generated by a speaker for $Re = 2938$ and $F_n = 10$ Hz and a) $F_e/F_n = 2.5$, b) $F_e/F_n = 4.5$, c) $F_e/F_n = 5.5$, and d) $F_e/F_n = 7.5$.



c)



d)

Fig. 8 Energy spectrum of acoustic waves generated by a speaker for $Re = 2938$ and $F_n = 10$ Hz and a) $F_e/F_n = 2.5$, b) $F_e/F_n = 4.5$, c) $F_e/F_n = 5.5$, and d) $F_e/F_n = 7.5$ (continued).

For the case of $Re = 8814$, to achieve synchronization of vortex shedding with the acoustic wave, the excitation frequency of the speaker must be much higher. Therefore, the energy spectrum of the acoustic wave generated by the speaker is expected to be much different from the case of $Re = 5876$ or 2938. Figure 10 shows that the maximum heat transfer occurs at $F_e/F_n = 4$, which is very close to the case of $F_e/F_n = 8$. The minimum in heat transfer enhancement occurs at $F_e/F_n = 7$. The large difference in heat transfer between the cases of $F_e/F_n = 7$ and 8 is attributed primarily to the different energy spectra of the acoustic waves. However, the decrease in sound pressure level does not change very much the entire energy

spectrum. This can be inferred from a similar kind of heat transfer enhancement at $Re = 8814$ with a lower sound pressure level, $S_{pl} = 90$ dB.¹⁸ The effect of sound pressure level on the heat transfer can be further understood using Fig. 11. In general, heat transfer enhancement is found to increase monotonically with increasing sound pressure level.

The average Nusselt number is defined as the average heat transfer coefficient multiplied by the diameter of the tube and divided by the thermal conductivity of the air. The average heat transfer coefficient is defined as the heat flux produced by the electric heater divided by the average temperature difference between the

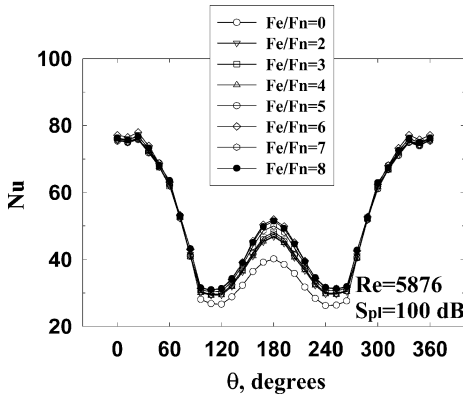


Fig. 9 Nusselt number distribution for $Re = 5876$ with acoustic excitation at $S_{pl} = 100$ dB.

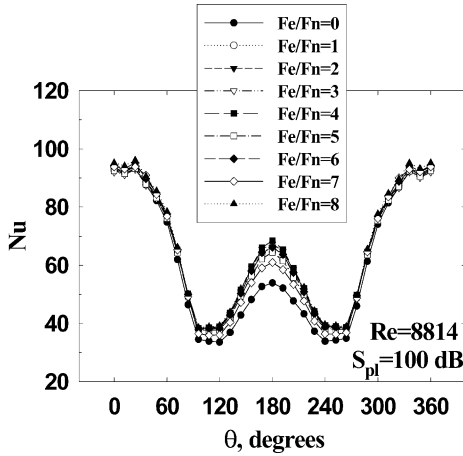
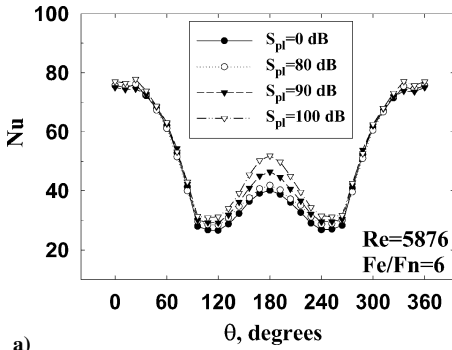
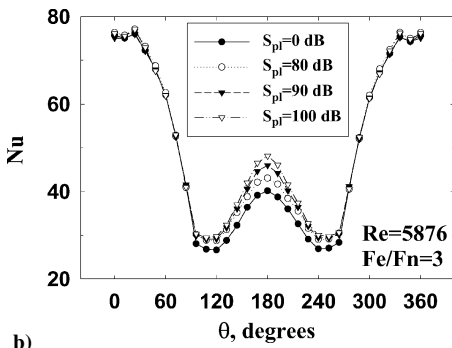


Fig. 10 Nusselt number distribution for $Re = 8814$ with acoustic excitation at $S_{pl} = 100$ dB.



a)



b)

Fig. 11 Nusselt number variation with sound pressure levels at a) $F_e/F_n = 3$ and b) $F_e/F_n = 6$.

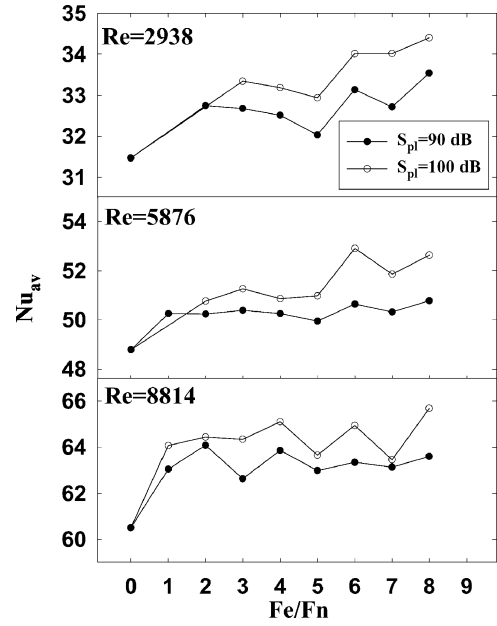


Fig. 12 Average Nusselt number variation with excitation frequency at frequencies from 0 to 8.

cylinder wall and the freestream air. The average Nusselt numbers at some selected excitation frequencies were found to increase with frequency for F_e/F_n from 0 to 8, as shown in Fig. 12. This may be attributed to the fact that a higher frequency excitation by an acoustic wave can provide more energy to disturb the flow and cause an earlier formation of the vortices and a greater enhancement in the heat transfer. A similar explanation has been given for the heat transfer enhancement due to cylinder oscillation.^{9,10} Higher heat transfer is found for cylinder oscillation at a higher synchronization frequency. However, this explanation could not be used for the current acoustic excitation since the energy spectrum of the acoustic waves generated by the current speaker varies significantly with excitation frequency. The decrease in the average Nusselt number with increasing the excitation frequency for F_e/F_n from 3 to 5, as shown in Fig. 12a and 12b, could not be explained by the previous statement, and should be explained from the results of energy spectrum measurements of the acoustic waves. In this region, the intensity or the sound level of the dominant mode of the frequency spectrum that causes synchronization with vortex shedding actually decreases with increasing the excitation frequency. This leads to a decrease in the heat transfer. The heat transfer starts to increase as the dominant mode of energy spectrum increases. The maximum heat transfer is found at $F_e/F_n = 8$ for $Re = 2938$ or 5876 , but at $F_e/F_n = 4$ for $Re = 8814$, where the intensity of the dominant mode of the frequency spectrum is the maximum. The acoustic excitation can amplify the instability, disturb the flow, and enhance the heat transfer, especially when synchronization occurs.

IV. Conclusions

The current experiments are performed for Re in the range from 2938 to 8814 with an acoustic excitation of S_{pl} from 0 to 100 dB and F_e/F_n from 0 to 8. Flow visualization has provided a clear vortex structure that grows more rapidly as the dominant mode of the instability in the shear layer is amplified by the excitation. Synchronization of vortex shedding with acoustic excitation can occur not only at all the harmonics or the superharmonics but also at some nonharmonics that can cause partial synchronization with vortex shedding, which can greatly enhance the heat transfer. However, enhancement in the heat transfer by earlier formation of vortices occurs only in the wake region of the cylinder. The enhancement of the heat transfer by the nonharmonic frequencies selected is much less than by the harmonics or the superharmonics. In addition, the heat transfer around the cylinder does not increase with increasing excitation frequency as was found for the case of heat transfer

enhancement by cylinder excitation, due to the input of more excitation energy at higher frequencies. More detailed measurements of the energy spectrum of the acoustic waves generated by the speaker are necessary for a better understanding.

Similar heat transfer enhancement by acoustic excitation is expected to occur at higher Reynolds numbers. However, the energy spectrum of the acoustic waves generated by the speaker will be altered significantly at a higher excitation frequency. This causes a significant variation in heat transfer enhancement with excitation frequency at higher Reynolds number. Despite this Reynolds number dependence, both the local and the average Nusselt number increase monotonically with sound pressure level.

Acknowledgment

This research was sponsored by the National Science Council of Taiwan under Contract NSC 90-2212-E-006-150.

References

- ¹Takahashi, K., and Endoh, K., "A New Correlation Method for the Effect of Vibration on Forced Convection Heat Transfer," *Journal of Chemical Engineering of Japan*, Vol. 23, No. 1, 1990, pp. 45–55.
- ²Fand, R. M., and Kaye, J., "The Influence of Sound on Free Convection from a Horizontal Cylinder," *ASME Journal of Heat Transfer*, Vol. 83, May 1961, pp. 133–148.
- ³June, R. R., and Baker, M. J., "The Effect of Sound on Free Convection Heat Transfer from a Vertical Flat Plate," *ASME Journal of Heat Transfer*, Vol. 85, Aug. 1963, p. 279.
- ⁴Richardson, P. D., "Heat Transfer from a Circular Cylinder by Acoustic Streaming," *Journal of Fluid Mechanics*, Vol. 30, Part 2, Nov. 1967, pp. 337–355.
- ⁵Fand, R. M., and Kaye, J., "The Influence of Sound on Heat Transfer from a Cylinder in Cross-Flow," *International Journal of Heat and Mass Transfer*, Vol. 6, No. 6, 1963, pp. 571–596.
- ⁶Gopinath, A., and Mills, A. F., "Convective Heat Transfer from a Sphere Due to Acoustic Streaming," *ASME Journal of Heat Transfer*, Vol. 115, No. 2, 1993, pp. 332–341.
- ⁷Gopinath, A., and Mills, A. F., "Convective Heat Transfer Due to Acoustic Streaming Across the Ends of a Kundt Tube," *ASME Journal of Heat Transfer*, Vol. 116, No. 1, 1994, pp. 47–53.
- ⁸Gau, C., Wu, J. M., and Liang, C. Y., "Heat Transfer Enhancement and Vortex Flow Structure over a Heated Cylinder Oscillating in Cross-Flow Direction," *ASME Journal of Heat Transfer*, Vol. 121, No. 4, 1999, pp. 789–795.
- ⁹Gau, C., Wu, S. X., and Su, H. S., "Synchronization of Vortex Shedding and Heat Transfer Enhancement over a Heated Cylinder Oscillating with Small Amplitude in Streamwise Direction," *ASME Journal of Heat Transfer*, Vol. 123, No. 6, 2001, pp. 1139–1148.
- ¹⁰Kline, S. J., and McClintock, F. A., "Describing Uncertainties in Single-Sample Experiments," *Mechanical Engineering*, Vol. 75, Jan. 1953, pp. 3–12.
- ¹¹Roshko, A., "On the Drag and Shedding Frequency of Two-Dimensional Bluff Bodies," NACA Technical Note, 1954, p. 3169.
- ¹²Zdravkovich, M. M., "Modulation of Vortex Shedding in the Synchronization Range," *ASME Journal of Fluid Engineering*, Vol. 104, No. 4, 1982, pp. 513–517.
- ¹³Blevins, R. D., "The Effect of Sound on Vortex Shedding from Cylinder," *Journal of Fluid Mechanics*, Vol. 161, Dec. 1985, pp. 217–237.
- ¹⁴Unal, M. F., and Rockwell, D., "On Vortex Formation from a Cylinder. Part 1. The Initial Instability," *Journal of Fluid Mechanics*, Vol. 190, May 1988, pp. 491–512.
- ¹⁵Krall, K. M., and Eckert, E. R. G., "Local Heat Transfer around Cylinder at Low Reynolds Number," *ASME Journal of Heat Transfer*, Vol. 94, No. 2, 1973, pp. 273–274.
- ¹⁶Griffin, O. M., and Ramberg, S. E., "Vortex Shedding from a Cylinder Vibrating in Line with an Incident Uniform Flow," *Journal of Fluid Mechanics*, Vol. 75, Part 2, 1976, pp. 257–271.
- ¹⁷Ongoren, A., and Rockwell, D., "Flow Structure from an Oscillating Cylinder, Part 2. Mode Competition in the Near Wake," *Journal of Fluid Mechanics*, Vol. 191, June 1988, pp. 225–245.
- ¹⁸Yang, Y. B., "Flow Structure and Heat Transfer over a Heated Cylinder Under Acoustic Excitation," M. S. Thesis, National Cheng Kung University, Tainan, Taiwan, Republic China, 2000.